Hysteresis in Combinatorial Optimization Problems

Yuling Guan[2] and **Ang Li**[1] and **Sven Koenig**[1] and **Stephan Haas**[2] and **T. K. Satish Kumar**[1,2,3]
[1]Department of Computer Science
[2]Department of Physics and Astronomy
[3]Department of Industrial and Systems Engineering
University of Southern California
{yulinggu, ali355, skoenig, shaas}@usc.edu, tkskwork@gmail.com

Abstract

Hysteresis is a physical phenomenon reflected in *macroscopic* observables of materials that are subjected to external fields. For example, magnetic hysteresis is observed in ferromagnetic metals such as iron, nickel and cobalt in the presence of a changing external magnetic field. In this paper, we model hysteresis using combinatorial models of *microscopic* spin interactions, for which we invoke the top K solution framework for Ising models and their generalizations, called Weighted Constraint Satisfaction Problems (WCSPs). We show that the WCSP model with a simple "memory effect" can be used to understand hysteresis *combinatorially* and from the perspective of statistical mechanics. In addition to the nearest neighbor interaction Ising model, the WCSP framework facilitates accurate simulations of long-range and k-body interactions between the spins.

Introduction and Motivation

Magnetic hysteresis is a physical phenomenon that occurs in many materials, especially in ferromagnetic metals such as iron, nickel and cobalt. It refers to the magnetic response of these materials to a changing external magnetic field that invokes a memory effect. Specifically, the total magnetization of the material follows one curve when the external magnetic field steadily increases and follows a different curve when it steadily decreases. Therefore, for the same value of the external magnetic field, the total magnetization of the material can have different possible values, depending on the history of the applied external magnetic field (Whittenburg, Dao, and Ross 2001). A typical hysteresis curve has an offset from the origin, is non-linear, and encloses a non-zero area between two saturation levels. Hysteresis can also occur in other macroscopic observables of materials that are subjected to external perturbations.

Although hysteresis is a physical phenomenon that can be characterized via precise measurements in controlled experiments, it is worth studying it theoretically and from a purely combinatorial perspective. In many ways, such a study would be similar to the study of phase transitions (Gent and Walsh 1994) and heavy-tailed phenomena (Gomes et al. 2000) in combinatorial problems. In statistical mechanics, macroscopic observables are related to the microscopic spin interactions via the Boltzmann distribution (Kardar 2007). However, this relationship is not always easy to study analytically. In fact, the difficulty in doing so is one of the reasons why hysteresis in macroscopic observables is still largely unexplained using microscopic models. In this paper, we show that, like phase transitions and heavy-tailed distributions, hysteresis too is an artifact of combinatorics, adding to the success of statistical mechanics. However, in order to show this, we propose a computational approach in lieu of an analytical approach and we make the reasonable assumption that the Boltzmann distribution, by virtue of being a negative exponential, is mostly concentrated on the lowest energy state and the first $K-1$ excited states, for some small K. To validate our approach, we invoke the top K solution framework for Weighted Constraint Satisfaction Problems (WCSPs) (Li et al. 2020) and show that the WCSP model with a simple "memory effect" can be used to understand hysteresis combinatorially and from the perspective of statistical mechanics. In this context, we also discuss how the memory effect is related to an effective "temperature" parameter.

While we first apply our methods to understand hysteresis in Ising models, compared to the nearest neighbor Ising model, our WCSP framework has the advantage of efficiently incorporating long-range and k-body interactions between the spins as well. Compared to other simulation frameworks, such as Monte Carlo methods, our WCSP framework has the advantage of using a principled statistical mechanics perspective. In addition, our WCSP framework allows us to understand hysteresis more generally in combinatorial optimization problems, with or without a connection to physically occurring phenomena.

Background

The Ising model (Lenz 1920) is a common model used in statistical mechanics where spins are restricted to

be ± 1. For the most part, research using Ising models has focused on pairwise interactions between nearest neighbor spins in a lattice structure. The pairwise interactions can be ferromagnetic or anti-ferromagnetic. A ferromagnetic interaction prefers the interacting spins to have the same value, while an anti-ferromagnetic interaction prefers the interacting spins to have opposite values. In an Ising model with periodic boundary conditions (PBCs), a particle on the boundary is considered as a nearest neighbor of its counterpart on the opposite boundary in the same dimension. PBCs are commonly used to emulate the behavior of infinite systems.

A spin configuration $\vec{\sigma}$ of the Ising model is an assignment of a ± 1 spin σ_i for each particle p_i in the lattice. The energy (Hamiltonian) of the spin configuration is

$$H(\vec{\sigma}) = -\mu_0 h \sum_{p_i} \sigma_i - J_{ij} \sum_{(p_i,p_j)\in E} \sigma_i \sigma_j, \tag{1}$$

where E represents the set of interacting nearest neighbor particles in the lattice structure. $J_{ij} > 0$ represents a ferromagnetic interaction; and $J_{ij} < 0$ represents an anti-ferromagnetic interaction. h represents the external magnetic field, and μ_0 is the magnetic permeability constant typically set to 1 in computational experiments. The total magnetization of the spin configuration $M(\vec{\sigma})$ is the number of spins which are set to $+1$ minus the number of spins which are set to -1.

The basic Ising model can be generalized by including more complex spin interactions. Interactions that are not restricted to nearest neighbor spins are called long-range interactions. Under various theoretical considerations, the long-range Ising model is typically described using the Hamiltonian (Zhang et al. 2008)

$$\begin{aligned} H(\vec{\sigma}) = &-\mu_0 h \sum_{p_i} \sigma_i - J \sum_{(p_i,p_j)\in E} \sigma_i \sigma_j \\ &+ D \sum_{p_i,p_j} \frac{\sigma_i \sigma_j - 3(\sigma_i \hat{y} \cdot \hat{r}_{ij})(\sigma_j \hat{y} \cdot \hat{r}_{ij})}{r_{ij}^3}, \end{aligned} \tag{2}$$

where $J_{ij} = J$ for all $(p_i, p_j) \in E$, and D is a dipolar coupling parameter. While the first term is defined over all nearest neighbor spins, the second term is a long-range interaction term defined over all pairs of spins. Its strength is inversely proportional to the cube of the distance, r_{ij}, between the interacting particles p_i and p_j. $\hat{r}_{ij}$ is the unit vector in the direction from p_i to p_j. $\hat{y}$ is the unit vector in the Y direction, assuming that all spins are ± 1 in that direction and the total magnetization is also measured in the Y direction. In general, D is relatively small compared to J.

The Ising model can also be generalized to include 3-spin interactions. In this model, each triplet of nearest neighbor spins that form a right angle interact via a 3-body term. The Hamiltonian of such a system is

$$\begin{aligned} H(\vec{\sigma}) = &-\mu_0 h \sum_{p_i} \sigma_i - J \sum_{(p_i,p_j)\in E} \sigma_i \sigma_j \\ &- J_3 \sum_{(p_i,p_j,p_k)\in L} \sigma_i \sigma_j \sigma_k, \end{aligned} \tag{3}$$

where J_3 is the 3-spin interaction parameter, and L contains all triplets (p_i, p_j, p_k) such that $(p_i, p_j) \in E$, $(p_j, p_k) \in E$ and $(p_i, p_j) \perp (p_j, p_k)$.

In statistical mechanics, the Boltzmann distribution is a probability distribution that specifies the probability of a system being in a certain state, i.e., in a spin configuration $\vec{\sigma}$, at a temperature T. The Boltzmann distribution is

$$P_\beta(\vec{\sigma}) = \frac{e^{-\beta H(\vec{\sigma})}}{Z_\beta}, \tag{4}$$

where $H(\vec{\sigma})$ is the energy of the spin configuration $\vec{\sigma}$, β is equal to $(k_B T)^{-1}$ for the Boltzmann constant k_B, and Z_β is a normalization constant, called the partition function, given by

$$Z_\beta = \sum_{\vec{\sigma}} e^{-\beta H(\vec{\sigma})}. \tag{5}$$

A macroscopic observable is the expected value of a function f defined on each possible spin configuration $\vec{\sigma}$. It is given by

$$\langle f \rangle = \sum_{\vec{\sigma}} P_\beta(\vec{\sigma}) f(\vec{\sigma}). \tag{6}$$

For example, in an Ising model where each spin is ± 1, $\langle M \rangle$ represents the total magnetization of a material when $M(\vec{\sigma})$ is defined to be the number of spins set to $+1$ minus the number of spins set to -1.[1]

Methodology

Magnetic hysteresis is observed in the total magnetization of a material when we apply an external magnetic field h according to a three-stage procedure: (Stage 1) $h \in [0, h_{max})$, (Stage 2) $h \in [h_{max}, -h_{max})$, and (Stage 3) $h \in [-h_{max}, h_{max}]$, where h_{max} is chosen to be much larger than the Ising coupling parameters J, J_3 and D.

Many experimental studies have been conducted to obtain hysteresis curves for different materials, including the CoO/Co film (Berger et al. 2000) and Nd-Fe-Al-B-Si alloys (Hadjipanayis and Gong 1988). There have also been many attempts to explain hysteresis mathematically using microscopic models. However, these methods use simplifying assumptions and are not very successful in matching the fundamental characteristic features of hysteresis curves. They are also unable to efficiently and effectively reason with long-range interactions and general k-body interactions for $k > 2$. In fact, although the Boltzmann distribution can be used to describe the relationship between the macroscopic observables and the microscopic spin models, it is not always easy to study it analytically. When faced with this analytical difficulty, methods that resort to approximations produce curves that compare poorly to those

[1] In the remainder of this paper, we simply write M as a short hand for the total magnetization $\langle M \rangle$. We also use m to represent the average magnetization, i.e., M divided by the total number of spins.

observed experimentally.[2]

A Monte Carlo algorithm is also often used as a baseline method to generate hysteresis curves (Wang et al. 2001). While this method has the benefit of producing curves that exhibit the fundamental characteristics of hysteresis curves observed experimentally for 2-dimensional lattices, the contours themselves may not exactly match those of the experimental curves. The Monte Carlo algorithm uses the Metropolis-Hastings importance sampling procedure (Newman and Barkema 1999) in its inner loop and works as follows.

In the beginning, i.e., for $h = 0$ in Stage 1, a spin configuration $\vec{\sigma}^*$ is generated by choosing each σ_i to be ± 1 uniformly at random. $M(\vec{\sigma}^*)$ is then reported as the total magnetization M. Henceforth, each time h changes, the algorithm starts an inner loop with L iterations to update $\vec{\sigma}^*$ and report the updated $M(\vec{\sigma}^*)$ as the new value of the total magnetization M. L is typically chosen to be one-third of the total number of spins. Iteration t of the inner loop constructs the spin configuration $\vec{\sigma}^t$, starting from $\vec{\sigma}^0$ set to $\vec{\sigma}^*$ computed for the previous value of h. $\vec{\sigma}^{t+1}$ is constructed from $\vec{\sigma}^t$ after the consideration of flipping a randomly chosen spin σ_i to obtain $\vec{\sigma}'$. If $H(\vec{\sigma}') < H(\vec{\sigma}^t)$, the flip is accepted and $\vec{\sigma}^{t+1}$ is set to $\vec{\sigma}'$. If not, the flip is accepted with probability $e^{\frac{H(\vec{\sigma}^t)-H(\vec{\sigma}')}{k_B T}}$.

The Monte Carlo algorithm incorporates the general idea that the repeated process of flipping chosen spins is equivalent to thermalizing a spin configuration with an environment of temperature T. It also incorporates the "memory effect" of hysteresis by simply setting $\vec{\sigma}^0$ to be $\vec{\sigma}^*$ in the inner loop.

The WCSP Top K Solution Framework

In this paper, we propose to study hysteresis by invoking the top K solution framework for WCSPs (Li et al. 2020). The WCSP is defined by a triplet $\mathcal{B} = \langle \mathcal{X}, \mathcal{D}, \mathcal{C} \rangle$, where $\mathcal{X} = \{X_1, X_2, \ldots, X_N\}$ is a set of N variables, $\mathcal{D} = \{D_1, D_2, \ldots, D_N\}$ is a set of N domains with discrete values, and $\mathcal{C} = \{C_1, C_2, \ldots, C_M\}$ is a set of M weighted constraints. Each variable $X_i \in \mathcal{X}$ can be assigned a value from its associated domain $D_i \in \mathcal{D}$. Each constraint $C_i \in \mathcal{C}$ is defined over a certain subset of the variables $S_i \subseteq \mathcal{X}$, called the scope of C_i. C_i associates a non-negative weight with each possible assignment of values to the variables in S_i. A solution $\mathcal{S}$ is an assignment of values to all variables in $\mathcal{X}$ from their respective domains. The top K solutions of a WCSP are a sequence of solutions $\mathcal{S}_1, \mathcal{S}_2, \ldots, \mathcal{S}_K$ such that $\mathcal{S}_k$, for $1 \leq k \leq K$, minimizes the sum of the weights specified by each weighted constraint in $\mathcal{C}$ and differs from each of $\mathcal{S}_1, \mathcal{S}_2, \ldots, \mathcal{S}_{k-1}$ in the value assigned to at least one variable.[3]

First, we note that the Hamiltonians described in each of Eq. (1), Eq. (2) and Eq. (3) can also be described using the language of weighted constraints as follows. We associate a Boolean variable with domain $\{-1, +1\}$ for each spin σ_i. A solution corresponds to a spin configuration $\vec{\sigma}$. The Hamiltonian terms involving individual σ_i's map to unary weighted constraints; the Hamiltonian terms involving $\sigma_i\sigma_j$'s map to binary weighted constraints; and the Hamiltonian terms involving $\sigma_i\sigma_j\sigma_k$'s map to ternary weighted constraints. Not only is the WCSP framework powerful enough to represent the Hamiltonians, but while traditional methods struggle with long-range and 3-spin interactions, these can also be very easily incorporated into the WCSP framework.

Second, we note that the lowest energy state maps to the optimal solution of the WCSP instance derived from the Hamiltonian. In fact, the lowest K energy states map to the top K solutions of the WCSP instance. Let Δ be the set of top K solutions to the WCSP instance. Using the reasonable assumption that the Boltzmann distribution, by virtue of being a negative exponential, is mostly concentrated on the lowest K energy states, for some small K, the partition function can be approximated as $Z_\beta = \sum_{\vec{\sigma} \in \Delta} e^{-\beta H(\vec{\sigma})}$ and the total magnetization can be approximated as $M = \sum_{\vec{\sigma} \in \Delta} P_\beta(\vec{\sigma}) M(\vec{\sigma})$. The top K solutions of WCSPs can be generated using the methods proposed in (Li et al. 2020). Such methods combine algorithmic techniques borrowed from artificial intelligence and operations research.

Third, we note that our approach uses a principled statistical mechanics perspective. It has been long argued that hysteresis occurs due to a "memory effect", i.e., a tendency of the system to remember and maintain its previous states in response to changes in the external magnetic field. This memory effect can be easily encoded in our WCSP framework using unary weighted constraints, making it significantly simpler than other methods that use differential equations. Our WCSP framework also allows us to understand hysteresis more generally in combinatorial optimization problems, with or without a connection to physically occurring phenomena.

Experiments and Analyses

In this section, we present our empirical results and analyses. Numerical experiments were conducted on a 3.6 GHz AMD Ryzen 5 3600 6-core CPU with 16 GB RAM. The top K solutions of WCSPs were generated using the Integer Linear Programming (ILP) formulation proposed in (Li et al. 2020). The ILPs were solved using Gurobi, while all other wrapper algorithms were implemented in Python 3.6. We used a 40×40 2-dimensional lattice structure with three different kinds

[2] The OOMMF (Object-Oriented Micro-Magnetic Frame) is an open-source software package aimed at developing portable and extensible public domain programs and tools for micro-magnetics (https://math.nist.gov/oommf/). It encapsulates a finite difference method to approximately solve the Landau-Lifshitz-Gilbert equation but it fails to match the experimental curves in fundamental characteristic features such as smoothness and slope (Whittenburg, Dao, and Ross 2001).

[3] $\mathcal{S}_1$ is referred to as an optimal solution or a top solution.

of spin interactions to generate our problem instances: nearest neighbor, long-range and 3-spin.

As noted earlier, the various terms of the Hamiltonians described in each of Eq. (1), Eq. (2) and Eq. (3) can be converted to weighted constraints. Similarly, simple unary constraints can be used to encode the memory effect in our WCSP framework. Suppose $\vec{\sigma}^1, \vec{\sigma}^2, \ldots, \vec{\sigma}^K$ are the top K spin configurations for a certain value of h. For the next value of h, unary constraints can be added to help the system "remember" these top K spin configurations. Each σ_i^j induces a unary constraint on the WCSP variable X_i corresponding to spin σ_i. The unary constraint assigns a cost of 0 for $X_i = \sigma_i^j$ and a cost of $\Gamma \frac{e^{-H(\vec{\sigma}^j)}}{Z}$ for $X_i \neq \sigma_i^j$, where $Z = \sum_{j=1}^{K} e^{-H(\vec{\sigma}^j)}$. Therefore, Γ measures the strength of the induced memory effect, and the other weighting factors are in accordance with the Boltzmann distribution. Later in this section, we examine the relationship between Γ and an effective temperature T.

Nearest Neighbor Spin Interactions

We first examine the empirical results on an Ising model with nearest neighbor ferromagnetic spin interactions. Fig. 1 shows these results on a 40×40 2-dimensional lattice structure with PBCs for different values of the memory effect parameter, Γ. Each spin only interacts with the external magnetic field h and its four nearest adjacent neighbors with strength J. The Hamiltonian of the system is as specified in Eq. (1), but with all J_{ij} set to J. As h begins to dominate J, m approaches saturation. That is, when h/J is high, m approaches 1, and when h/J is low, m approaches -1. Higher values of Γ induce more memory. As Γ increases, the curves begin to exhibit the characteristic features of hysteresis curves, and the area enclosed between the Stage 2 and Stage 3 contours of the hysteresis curves also increases. Physically, this enclosed area represents the energy required from the external magnetic field to flip spins, and as expected, higher values of Γ induce more memory and thereby increase this required energy. The slopes of the Stage 2 and Stage 3 contours also decrease with increasing Γ for the same reason.

Memory Effect and Temperature

As noted earlier, the baseline Monte Carlo algorithm incorporates a general intuition about the dynamics of changing h in relationship to the temperature. On the other hand, our WCSP approach uses a principled statistical mechanics perspective. While our WCSP approach uses Γ to induce a memory effect in the system, the Monte Carlo algorithm incorporates it by setting $\vec{\sigma}^0$ to be $\vec{\sigma}^*$ in its inner loop but subsequently thermalizes it with temperature T. In this subsection, we examine whether Γ and T are possibly related to each other. An inverse relationship is certainly conceivable from a physical standpoint because particles are more stable at lower temperatures compared to higher temperatures; and so, it is harder to flip spins when the temperature decreases, leading to a larger memory effect.

To unravel a possible relationship between Γ and T, we run our WCSP algorithm as well as the Monte Carlo algorithm on the same 40×40 2-dimensional lattice structure with PBCs. We match values of Γ with those values of T that yield the same enclosed areas between the Stage 2 and Stage 3 contours. This is because this area is the most important comparative feature since it reflects an energy consideration on the system that measures the cost of flipping spins. For example, Fig. 2(a) is generated using the Monte Carlo algorithm with T set to $0.8J$, and its enclosed area matches that of Fig. 1(c).

By using the enclosed area between the Stage 2 and Stage 3 contours of hysteresis curves as a bridge between our WCSP algorithm and the Monte Carlo algorithm, we can plot data points indicating the relationship between Γ and T, as shown in Fig. 2(b). We then fit an allometric power function on these data points to yield the best-fit curve given by $\Gamma = 6.24 \times T^{-1.04}$. Indeed, this inverse relationship is close to what is expected from physical intuition: At lower temperatures, the effect of memory is stronger.

Long-Range Spin Interactions

In this subsection, we examine empirical results on an Ising model with long-range ferromagnetic spin interactions. Fig. 3 shows these results on a 40×40 2-dimensional lattice structure with PBCs for $K = 4$ and $\Gamma = 8$. Each spin interacts with the external magnetic field h, each of its four nearest adjacent neighbors with strength J, and every other spin with strength D/r^3, where r is the distance between the interacting spins. The Hamiltonian of the system is as specified in Eq. (2).

Fig. 3(a) shows the effect of long-range interactions on the hysteresis curve when $D/J = 0.2$ and $\Gamma = 8$. We first note that this curve has all the characteristic features of a hysteresis curve obtained through physical experiments. However, compared to the hysteresis curve in Fig. 1(c) produced by the nearest neighbor Ising model under the same parameter values, the hysteresis curve in Fig. 3(a) is marginally smoother and has a marginally smaller area enclosed between the Stage 2 and Stage 3 contours. This is because long-range interactions, although weaker than nearest neighbor interactions, reinforce them since they too are ferromagnetic; and because D and J have opposite signs in Eq. (2), this effectively decreases J and increases h/J. This makes it easier to flip spins, leading to smoother hysteresis curves and smaller areas enclosed between the Stage 2 and Stage 3 contours, as explained before via energy considerations.

The geometry of a hysteresis curve is typically symmetric around the Y-axis; and four interesting points in this geometry are $(-H_s, -1)$, $(-H_c, 0)$, $(+H_c, 0)$ and $(+H_s, +1)$. Fig. 3(b) shows the behavior of the values of H_c and H_s as D/J varies for $K = 4$ and $\Gamma = 8$. With increasing D/J, the value of H_c mostly stays the same, fluctuating within the narrow range

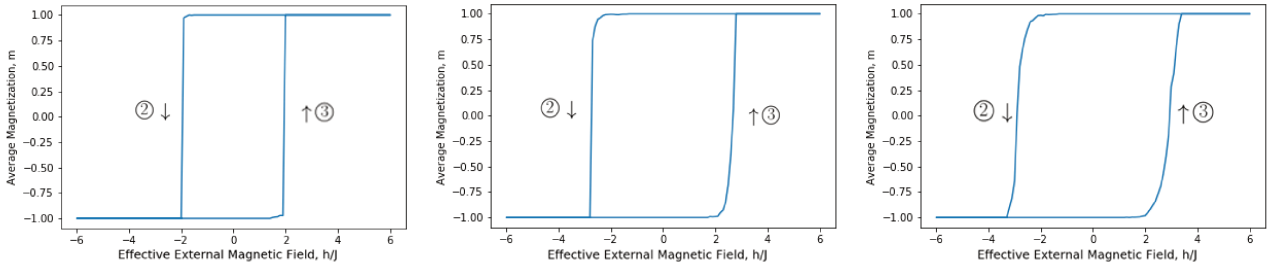

(a) $\Gamma = 4$ (b) $\Gamma = 6$ (c) $\Gamma = 8$

Figure 1: Shows the hysteresis curves for different values of Γ on a 40×40 2-dimensional lattice structure with PBCs and nearest neighbor ferromagnetic spin interactions. K is set to 8 in all cases. The X-axis represents the effective external magnetic field, h/J, and the Y-axis represents the average magnetization, m. Each curve includes the second and third stages of hysteresis marked by ② and ③, respectively.

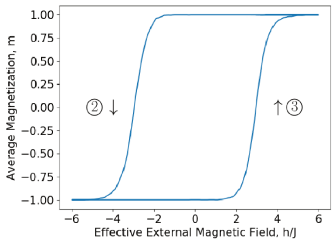

(a) Monte Carlo Hysteresis

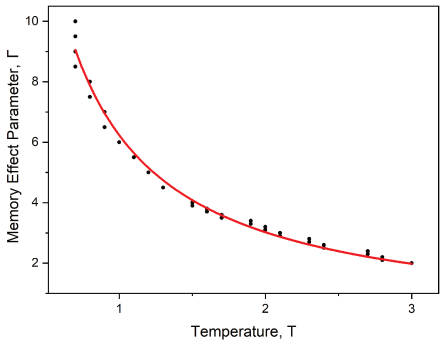

(b) Γ vs T

Figure 2: (a) shows the hysteresis curve obtained by the baseline Monte Carlo algorithm for the same 40×40 2-dimensional lattice structure with PBCs and nearest neighbor ferromagnetic spin interactions used in Fig. 1. The temperature T is set to $0.8J$ to match the enclosed area between the Stage 2 and Stage 3 contours with that of Fig. 1(c). (b) shows the best-fit curve for unraveling a possible relationship between Γ and T. In general, $\Gamma \propto T^{-1}$.

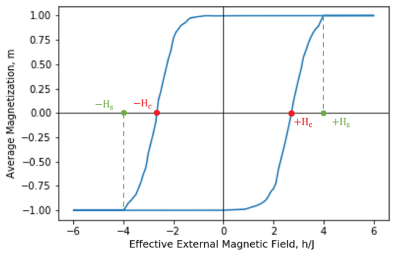

(a) Long-Range Hysteresis

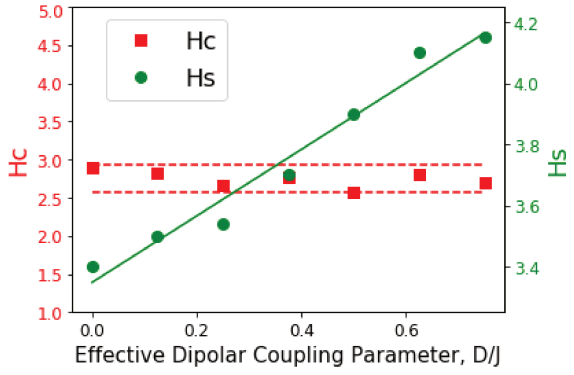

(b) H_c and H_s vs D/J

Figure 3: (a) shows the hysteresis curve for a 40×40 2-dimensional lattice structure with PBCs and long-range ferromagnetic spin interactions. The effective dipolar coupling parameter $D/J = 0.2$. (b) shows the dependence of H_c and H_s on D/J. $\pm H_c$ are the critical values of h when m is 0; and $\pm H_s$ are the saturation values of h when m first hits ± 1, respectively. H_c is indicated in red with a scale on the left margin, while H_s is indicated in green with a scale on the right margin. K is set to 4 and Γ is set to 8 in all cases.

$[2.8, 3.0]$, shown in red. On the other hand, H_s increases proportionally to D/J, according to the best-fit curve $H_s = 1.08D/J + 3.34$, shown in green. Additionally, as argued before, the area enclosed between the Stage 2 and Stage 3 contours decreases with increasing D/J.

3-Spin Interactions

The Hamiltonian of a 3-spin system is as specified in Eq. (3). Our WCSP framework allows for the incorporation of 3-spin and general k-body interactions as higher-arity weighted constraints. Fig. 4 shows the

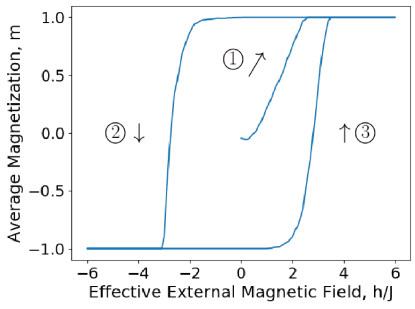

(a) $J_3/J = 0.1$

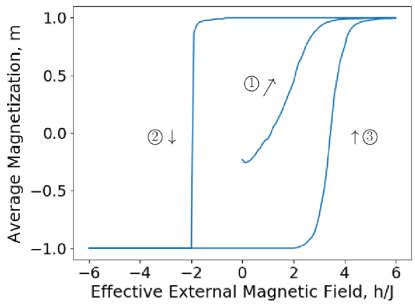

(b) $J_3/J = 0.5$

Figure 4: Shows the hysteresis curves for a 40×40 2-dimensional lattice structure with PBCs and 3-spin interactions, for two different values of J_3/J. K is set to 1 and Γ is set to 8. Each curve includes the three stages of hysteresis.

effective magnetic field h/J on the X-axis and the average magnetization m on the Y-axis, for different values of J_3/J. We used Toulbar2 (Hurley et al. 2016) as our WCSP solver since it is suitable for such higher-arity weighted constraints. However, higher-order interactions are not popularly studied in physics. Therefore, we presently cannot draw any important conclusions or parallels between higher-order spin systems and combinatorial optimization problems with respect to hysteresis. In future work, we will investigate whether 3-spin interactions can explain meta-stable states and phase transitions in spin systems and whether they can be validated through our WCSP approach. As can be seen in Fig. 4, this is a plausibility since larger values of J_3/J begin to induce steeper Stage 2 contours, perhaps indicative of meta-stable states.

Conclusions and Future Work

Hysteresis is a well-known physical phenomenon in the macroscopic world. However, methods to explain hysteresis using microscopic spin interactions have not been very successful. In this paper, we proposed a method based on the top K solution framework for WCSPs. Our methodology has several benefits. First, it uses a principled statistical mechanics perspective. Second, it incorporates the memory effect using simple unary weighted constraints, parameterized by a factor Γ that was experimentally verified to be proportional to the inverse of the temperature. Third, it generates curves that have all the fundamental characteristics of experimental hysteresis curves. Fourth, it supports long-range and k-body interactions. Overall, our WCSP method allows us to understand hysteresis more generally in combinatorial optimization problems, with or without a connection to physically occurring phenomena. We also believe that our paper is the first attempt to explain hysteresis using the top K solution framework for WCSPs. Therefore, there are many avenues possible for future work. One important direction is to make the top K solution framework more efficient. A second direction is to use richer models like quantum spin interactions.

References

[Berger et al. 2000] Berger, A.; Inomata, A.; Jiang, J. S.; Pearson, J. E.; and Bader, S. D. 2000. Experimental observation of disorder-driven hysteresis-loop criticality. *Phys. Rev. Lett.* 85:4176–4179.

[Gent and Walsh 1994] Gent, I., and Walsh, T. 1994. The SAT phase transition. In *Proceedings of the European Conference on Artificial Intelligence*.

[Gomes et al. 2000] Gomes, C.; Selman, B.; Crato, N.; and Kautz, H. 2000. Heavy-tailed phenomena in satisfiability and constraint satisfaction problems. *Journal of Automated Reasoning* 24:67–100.

[Hadjipanayis and Gong 1988] Hadjipanayis, G. C., and Gong, W. 1988. Magnetic hysteresis in melt-spun Nd-Fe-Al-B-Si alloys with high remanence. *Journal of Applied Physics* 64(10):5559–5561.

[Hurley et al. 2016] Hurley, B.; O'sullivan, B.; Allouche, D.; Katsirelos, G.; Schiex, T.; Zytnicki, M.; and Givry, S. D. 2016. Multi-language evaluation of exact solvers in graphical model discrete optimization. *Constraints* 21(3):413–434.

[Kardar 2007] Kardar, M. 2007. *Statistical Physics of Particles*. Cambridge: Cambridge University Press.

[Lenz 1920] Lenz, W. R. 1920. Beitrag zum verständnis der magnetischen erscheinungen in festen körpern. *Physikalische Zeitschrift* 21:613–615.

[Li et al. 2020] Li, A.; Guan, Y.; Koenig, S.; Haas, S.; and Kumar, T. K. S. 2020. Generating the top K solutions to weighted CSPs: A comparison of different approaches. In *Proceedings of the IEEE International Conference on Tools with Artificial Intelligence*.

[Newman and Barkema 1999] Newman, M. E. J., and Barkema, G. T. 1999. *Monte Carlo Methods in Statistical Physics*. Oxford: Clarendon Press.

[Wang et al. 2001] Wang, L.; Ding, J.; Kong, H. Z.; Li, Y.; and Feng, Y. P. 2001. Monte carlo simulation of a cluster system with strong interaction and random anisotropy. *Phys. Rev. B* 64.

[Whittenburg, Dao, and Ross 2001] Whittenburg, S. L.; Dao, N.; and Ross, C. A. 2001. Micromagnetic studies of hysteresis in nickel pillars. *Physica B: Condensed Matter* 306(1):44–46.

[Zhang et al. 2008] Zhang, W.; Singh, R.; Bray-Ali, N.; and Haas, S. 2008. Scaling analysis and application: Phase diagram of magnetic nanorings and elliptical nanoparticles. *Phys. Rev. B* 77.